Regulation of Methane Monooxygenase Catalysis Based on Size Exclusion and Quantum Tunneling†

Hui Zheng and John D. Lipscomb*

Department of Biochemistry, Molecular Biology, and Biophysics and Center for Metals in Biocatalysis, University of Minnesota, Minneapolis, Minnesota 55455

Received August 11, 2005; Revised Manuscript Received December 13, 2005

ABSTRACT: The hydroxylase component (MMOH) of the soluble form of methane monooxygenase (sMMO) isolated from *Methylosinus trichosporium* OB3b catalyzes both the O_2 activation and the CH_4 oxidation reactions at the oxygen-bridged dinuclear iron cluster present in its buried active site. During the reaction cycle, the diiron cluster forms a bis-μ-oxo-(Fe(IV))$_2$ intermediate termed compound Q (Q) that reacts directly with methane. Many adventitious substrates also react with Q, most at a relatively slow rate. We have proposed that Q reacts preferentially with CH_4 because the sMMO regulatory component MMOB induces a size selective pore into the MMOH active site as the two components form a complex. Support for this proposal has come through the observation of a nonlinear Arrhenius plot for the CH_4 oxidation, presumably due to a shift in rate-limiting step from substrate binding at low temperature to C−H bond cleavage at high temperature. Reactions of all substrates other than CH_4 fail to exhibit a break in the Arrhenius plot because binding is always rate limiting in the temperature range explored. Here we show that it is possible to induce a break in the Arrhenius plot for the ethane reaction with Q by using an MMOB mutant termed DBL2 (S109A/T111A) in which residues at the MMOH−MMOB interface are reduced in size. We hypothesize that this increases the ethane binding rate and shifts the Arrhenius breakpoint into the observable temperature range. As a result of this shift, the kinetic and activation parameters of the C−H bond breaking reaction for both methane and ethane can be observed using the DBL2 mutant. A ^{2}H-KIE is observed for both substrate oxidation reactions when using DBL2, whereas only CH_4 oxidation exhibits an effect when using wild type MMOB, consistent with the C−H bond cleaving reaction becoming at least partially rate limiting for ethane. Analysis of the temperature dependence of the ^{2}H-KIE for ethane and methane for reactions using both mutant and wild type forms of MMOB suggests that quantum tunneling plays a significant role in methane oxidation but not ethane oxidation.

Methane monooxygenase (MMO[1]) isolated from methanotrophic bacteria catalyzes the first step of the oxidative degradation of methane, the conversion of methane to methanol (*1*).

$$NAD(P)H + H^+ + CH_4 + O_2 \rightarrow NAD(P)^+ + CH_3OH + H_2O$$

The soluble MMO system isolated from *Methylosinus trichosporium* OB3b consists of three protein components: a hydroxylase (MMOH), a reductase (MMOR), and a regulatory protein termed component B (MMOB) (*2*). Our past studies have shown that both the O_2 activation and the methane oxidation reactions are catalyzed by MMOH which contains an oxygen-bridged diiron cluster in the active site of each α-subunit of the $(\alpha\beta\gamma)_2$ enzyme (*3*−*5*). MMOB regulates the reaction by forming a stoichiometric complex with the α-subunits of the MMOH (*6*).

Detailed studies of the kinetics of the reaction cycle of MMOH have revealed several transient intermediate species (*4*, *7*−*9*) as illustrated in Scheme 1. The cycle is conveniently described as consisting of an oxygen activation phase followed by a hydrocarbon reaction phase (*4*, *10*, *11*). During oxygen activation, the diiron cluster is first reduced from the diferric (H^{ox}) to the diferrous (H^r) state by the NAD(P)H-reduced MMOR or by a chemical reducing agent such as dithionite. Then, in the presence of MMOB, the diferrous MMOH reacts rapidly with O_2, forming an oxygen adduct (O), a peroxo or superoxo species (P*), and finally a hydroperoxo species (P) before forming a novel bis-μ-oxo-Fe(IV)$_2$ intermediate termed compound Q (Q). Q is the species that completes the O_2 activation phase and initiates the hydrocarbon reaction phase. It is capable of reacting with unactivated hydrocarbons to form the product alcohol complex in the active site, termed compound T (T). The

† This work was supported by NIH Grant GM40466.

* Author to whom correspondence should be addressed. Department of Biochemistry, Molecular Biology, and Biophysics, 6-155 Jackson Hall, 321 Church St. SE, University of Minnesota, Minneapolis, MN 55455. Tel: (612) 625-6454. Fax: (612) 624-5121. E-mail: lipsc001@umn.edu.

[1] Abbreviations: MMO, methane monooxygenase; sMMO, soluble form of methane monooxygenase; MMOH, sMMO hydroxylase component; MMOB, sMMO component B; MMOR, sMMO reductase; WT-MMOB, wild-type MMOB; Quad mutant, MMOB mutant N107G/S109A/S110A/T111A; DBL2, MMOB mutant S109A/T111A; MOPS, 3-[*N*-morpholino]propane-sulfonic acid; H^{ox}, oxidized MMOH; H^r, reduced MMOH; O, P*, P, Q, R, T, compounds O, P*, P, Q, R, and T from the MMOH catalytic cycle; d_4-methane, fully deuterated methane; d_6-ethane, fully deuterated ethane; HTR and LTR, high and low temperature regions, respectively, of a nonlinear Arrhenius plot.

10.1021/bi051605g CCC: $33.50
Published on Web 01/19/2006

Scheme 1: Intermediates in a Single Turnover Reaction of Diferrous MMOH

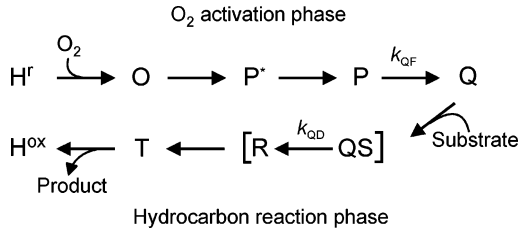

mechanism of this reaction remains a topic of study (*11*, *12*), but it may involve a substrate radical intermediate termed compound R (R).

MMOB has been shown to play a very significant role in many steps of this cycle. The complex of MMOB with MMOH alters the redox potential for electron transfer to the diiron cluster (*13*, *14*). Also, the regiospecificity for hydroxylation of substrates more complex than methane is strongly affected by the presence of MMOB, suggesting that it is able to alter the structure of the MMOH active site (*15*). An early indication of perhaps the most significant role of MMOB was the fact that O_2 reacts to form P* 1000 times faster when MMOB is present (*8*). As a result, the rate-limiting step shifts from the first to the last step of the cycle allowing the intermediates to be detected.

The X-ray crystal structure of MMOH has been solved and shows that the active site is buried with no obvious access channel (*5*, *16*, *17*). Recently, xenon trapped in the crystal has been used to attempt to detect an access route for small molecules into the site (*18*). While a convoluted path can be described, it is clearly not an open channel as utilized by most enzymes that metabolize O_2. Moreover, spectroscopic studies have shown that the active site structure is altered by the formation of the MMOB−MMOH complex, suggesting that the entry route for small molecules may also change (*6*, *19*, *20*).

NMR solution structures of MMOB have also been solved, and the interface surface with MMOH has been described (*21*−*23*). Remarkably, mutagenesis of specific MMOB residues on the interaction surface affected the rate constants for specific steps in the reaction cycle (*24*). At least five steps are affected by specific MMOB mutations; thus, MMOB regulates catalysis throughout the cycle. One 4-residue mutation MMOB (N107G/S109A/S110A/T111A), termed the Quad mutant, was found to accelerate the reaction of large substrates with Q and also accelerate the release of large products. Based on this observation, a "molecular sieve" hypothesis for the mechanism of action of MMOB was developed (*24*−*26*). It was proposed that the MMOB−MMOH complex resulted in formation of a pore (or a change in interface residue mobility) into the active site of MMOH that is able to select methane and O_2 on the basis of size. This provides one route to specificity for sMMO that allows methane to be preferentially oxidized in the presence of substrates that have weaker C−H bonds and, consequently, might be expected to react more rapidly. The Quad mutant presumably opens the pore further by placing smaller residues at the entrance.

The Quad mutant had the unexpected effect of decreasing the rate constant specifically for reaction of Q with methane. Interestingly, this was only the case for methane and not d_4-methane, resulting in a decrease in the KIE for the reaction from ∼50 when WT-MMOB was used (*27*) to ∼6 when Quad mutant MMOB was used (*25*). It was proposed that the normal reaction of methane with Q proceeds with a large quantum tunneling component which is compromised in some way when the MMOB−MMOH interface is perturbed. Since a KIE >1 and tunneling are only observed for methane, this provides a second level of selectivity for the natural substrate. Such selectivity is essential because methane is the only growth substrate for methanotrophs.

The nature of the reaction of Q with substrates has been studied as a function of temperature. It was found that a break is observed in the Arrhenius plot specifically for the methane reaction indicative of at least a two-step process (*9*). All other substrates, including CD_4, gave linear plots. We proposed that the reaction occurs by first binding substrates to Q to form intermediate QS and then insertion of oxygen from Q into the substrate C−H bond. Due to the small channel into the active site, the binding is rate limiting throughout the observable temperature range for most substrates. In the case of methane, the small size and strong C−H bond allow C−H bond cleavage to become rate limiting at a temperature between 10 and 20 °C, leading to the observed break in the Arrhenius plot.

The Quad mutant and other mutants based on it have been useful in exploring both the molecular sieve hypothesis and the proposed two-step nature of the Q reaction. In particular, it was shown that use of the Quad mutant caused the rate constant for the reaction of Q with ethane to increase while that for d_6-ethane remained unchanged, thereby unmasking the isotope effect (*25*). This was presumably due to an increase in the rate constant for binding allowing the bond-breaking reaction to become rate limiting.

At present, the two-step nature of the Q reaction with substrates and the molecular sieve hypothesis rest primarily on the observation of the Arrhenius plot break for only a single substrate, methane. Also, the proposals for quantum tunneling in sMMO are dependent on observations for methane oxidation because it is the only substrate for which the C−H bond cleavage can apparently be made rate limiting. The ability to unmask the isotope effect for ethane using the Quad mutant suggests that the activation energies for binding and bond breaking must be similar for this substrate such that a break in the Arrhenius plot might be observed under the correct conditions. The Quad mutant is not sufficiently stable to use in the large-scale kinetic study required. Consequently, in this study, we explore the reactions of Q with substrates using a much more stable and easily prepared variant of the Quad mutant called DBL2 (S109A/T111A) (*26*). These studies confirm and extend our model for the regulation and mechanism of the reaction of the key intermediate in sMMO catalysis.

EXPERIMENTAL PROCEDURES

Enzyme Purification. MMOH was purified as previously described from *M. trichosporium* OB3b (*2*, *28*). Recombinant MMOB and DBL2 mutant were purified as previously described (*22*, *24*, *26*).

Chemicals. All chemicals were purchased from Sigma, Aldrich, or Cambridge Isotope Laboratories and used without purification. Water was deionized and then purified using a

Millipore reverse osmosis system. Methane and ethane solutions were prepared by bubbling gas for 1 h into 1 mL of 50 mM MOPS, pH 7. The solutions were previously determined to be saturated after this period by GC analysis (*25*, *27*). The concentrations of the saturated methane and ethane solutions were 1.5 mM and 2.1 mM, respectively, at 25 °C (Merck Index). Solutions of varied substrate concentrations were then made by dilutions from the saturated solutions using a gastight syringe so that the solutions were not exposed to a headspace prior to loading into the stopped-flow apparatus. Deuterated substrates are 1−2% less soluble than their counterparts in aqueous media, leading to a correction which is small relative to the overall differences in rate constants observed.

Stopped-Flow Experiments. Single-turnover reactions of MMOH were monitored using a stopped-flow apparatus from Applied Photophysics (model SX.18MV). The sample preparation has been reported previously (*25*). In brief, MMOH was made anaerobic and subsequently reduced with methyl viologen and stoichiometric dithionite to yield the 2 electron reduced state. It was then transferred to the stopped-flow apparatus using a Hamilton gastight syringe. The other stopped-flow syringe was loaded with MMOB in oxygen-saturated (∼1.4 mM) buffer and the appropriate substrate. The samples were then rapidly mixed (1:1), and the absorbance changes were followed at a fixed wavelength. The mixed concentration of MMOH was 23 μM active sites and that of the WT-MMOB or DBL2 mutant was 25 μM. The buffer for all experiments was 50 mM MOPS, pH 7. In temperature dependent experiments, the temperature was adjusted by a circulating water bath. Before rapidly mixing at a new temperature, the samples were allowed to equilibrate for 15 min.

Data Analysis. Pseudo-first-order kinetics were generally observed because O_2 adds in an effectively irreversible step in the dead time of the stopped-flow instrument for all experiments and the hydrocarbon substrate concentrations are in large excess over that of MMOH for most experiments. The reactions consisted of two or more steps, resulting in two or more kinetic phases in the time course. The phases sum together to reproduce the overall time course. The number of relaxations observed defines the minimum number of steps in the reaction, but it does not define a specific mechanism or order for the steps. In the current case, rapid scan optical and time-resolved Mössbauer spectroscopies (*4*, *29*, *30*) have shown that P forms prior to Q. If it is assumed that the steps are irreversible, then the relaxation times are equal to the reciprocal rate constants for the steps. Finally, amplitude analysis has been used to identify which relaxation time is associated with the formation of Q (*4*). The reciprocal relaxation times (RRTs) and the amplitudes of each phase were determined using the nonlinear regression fitting program KFIT developed by Neil C. Millar (King's College London, U.K.). At least 10 repeated measurements of each time course for a given set of conditions were collected and individually fit. The fit values were then averaged to give an RRT value and a statistical error value. This process was repeated at least three times with different enzyme batches on different days.

The assignment of the RRTs determined using a summed three exponential fit at 430 nm for the reaction sequence leading to Q formation and decay was based on the observation that only the rate of Q decay has been shown to be accelerated by the presence of substrates (*27*, *30*).[2] Thus, as the concentration of substrate was varied, the rate constant of Q decay was identified as the reciprocal relaxation time that changed while the other two rate constants were assigned to Q and P (or P*) formation.

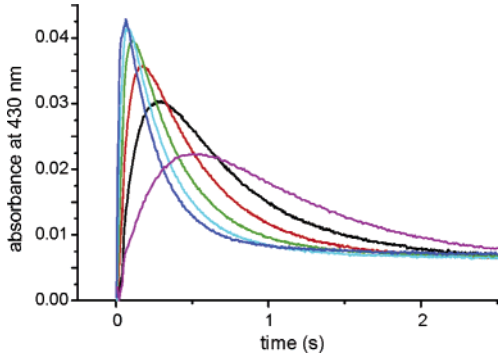

FIGURE 1: Time course of Q formation and decay of DBL2 with 200 μM methane as a function of temperature. The reaction was monitored at 430 nm in a stopped-flow spectrophotometer with a single wavelength detector at pH 7.0. The temperature range is from 4 °C (purple) to 24 °C (dark blue) with a 4 °C increment between the time courses shown.

Temperature-Dependent Analysis. The natural log of the rate constants for each averaged set of experimental data were plotted against the reciprocal of the absolute temperature. In the case of Q decay, a second-order rate constant was used as determined from the slope of the apparent first-order rate constant versus methane concentration plot. The data were then fit to the Arrhenius equation (eq 1) using the linear fitting function in the plotting program Origin (OriginLab) or Excel (Microsoft), and the error from this fit is reported in the tables. In this equation, A is the Arrhenius preexponential factor and R is the gas constant. The position of the breakpoint in the nonlinear Arrhenius plots was found by fitting the high and low temperature regions of the Arrhenius plot separately.

$$\ln k = \ln A - E_a/RT \quad (1)$$

The activation enthalpy, activation entropy, and Gibbs free energy of activation were determined using eqs 2, 3, and 4, respectively, where k_B is the Boltzmann constant and h is Planck's constant.

$$\Delta H^{\ddagger} = E_a - RT \quad (2)$$

$$\Delta S^{\ddagger} = R(\ln A - \ln(k_B T/h)) \quad (3)$$

$$\Delta G^{\ddagger} = \Delta H^{\ddagger} - T\Delta S^{\ddagger} \quad (4)$$

RESULTS

Overall Reaction Time Course. The ability of DBL2 to promote the interconversion of MMO reaction cycle intermediates was examined using transient kinetic techniques for comparison with past studies using WT-MMOB. The overall changes in the time courses of the formation and decay of Q in the presence of DBL2 at different temperatures are shown in Figure 1. The fact that the maximum concentration of Q (Q_{max}) increases with increasing temperature shows that the formation rate constant (k_{QF}) increases faster

than the decay rate constant (k_{QD}). Thus, the activation energy for Q formation is larger than that for Q decay as previously found when using WT-MMOB (Tables S1 and S2, Supporting Information). However, a larger Q_{max} is observed when using DBL2 in place of WT-MMOB as a result of a similar Q formation rate constant but a somewhat slower Q decay rate constant at any given temperature.

Temperature Dependence and the Effect of Substrate on Q Formation. Previous studies of the effect of temperature on the rate constant for Q formation using the components from the *M. trichosporium* MMO system have failed to reveal a significant dependence on substrate type or concentration (*4*, *25*).[3] Similarly, the linear Arrhenius plot of Q formation using DBL2 reveals the same activation energy (Table S1) within error for all tested substrates and when substrate is omitted from the reaction.

Effect of Methane Concentration on the Temperature Dependence of Q Decay. Figure 2A shows the effect of methane concentration on the temperature dependence of the k_{QD} measured using DBL2 under the same reaction conditions as used for the formation reaction described above. These reactions exhibited the same characteristics as the previously investigated reactions using WT-MMOB, specifically (i) linear Arrhenius plots when no substrate or 50 μM methane is present, (ii) nonlinear Arrhenius plots at higher methane concentrations, and (iii) an increase in the temperature of the breakpoints in the Arrhenius plots as the methane concentration increases. The observed plots at temperatures above or below the breakpoints appear linear as represented in the data sets of 200 μM methane reactions. The breakpoints using DBL2 in place of WT-MMOB shift to slightly lower temperature, and the reaction is slower at all temperatures shown in Figure 2B. Alternative causes for the nonlinearity of these plots such as thermal inactivation, protein-conformation change, or a pH change of buffer with temperature have been ruled out in previous studies (*25*).

We have previously proposed that the C−H bond breaking step is rate limiting in the high temperature region (HTR) to the left of the break based on comparisons of the activation parameters for methane and other substrates (*25*). If this is correct, then a linear plot might be expected for d_4-methane where the stronger bond would shift the breakpoint to lower temperature, out of the observable range. This reaction using DBL2 was investigated over a large range of d_4-methane concentrations and found to give linear Arrhenius plots using either the pseudo first order or second order rate constants for Q decay as shown in Figure 3. Despite changes in rate constants and activation parameters (Table S2), the reactions of methane with Q using DBL2 are generally similar to those using WT-MMOB. This is expected based on the hypothesis that the pore into the active site of MMOH is big enough for methane when using WT-MMOB and is only made bigger using DBL2. In contrast, substantial differences are observed when ethane is used as the substrate as described below.

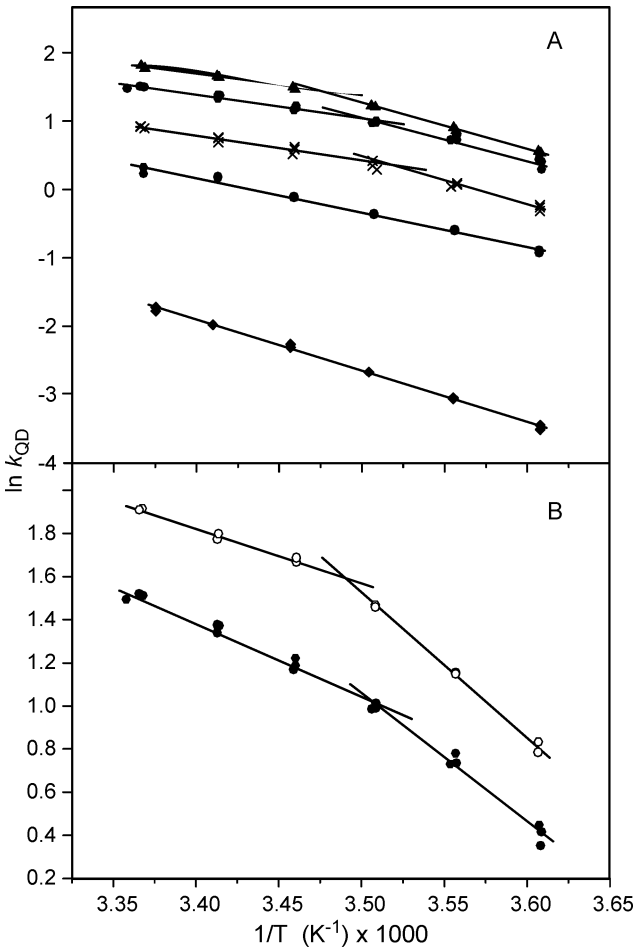

FIGURE 2: Q decay reaction in the presence of DBL2. Panel A: Arrhenius plots of the reaction at various methane concentrations. From bottom to top, no substrate, 50 μM, 100 μM, 200 μM, 300 μM methane. Panel B: Arrhenius plots for the Q decay reaction in the presence of 200 μM methane in reactions using DBL2 (●), WT-MMOB (○). For both panels, 3 typical data sets are superimposed to indicate the reproducibility of the experiment.

Effect of Ethane Concentration on the Temperature Dependence of Q Decay. Figure 4A shows that when DBL2 is used, the Arrhenius plots for k_{QD} exhibit a distinct break at d_6-ethane concentrations over 100 μM. Breaks are also observed when ethane is used; an example of this is seen in Figure 4B. When using WT-MMOB, this reaction shows only linear Arrhenius plots (Figure 4B) and no deuterium KIE (*25*). The change in the temperature of the breakpoints with substrate concentration is much greater than that observed when using methane as the substrate (compare Figures 2A and 4A). In fact, extrapolation of the breakpoint temperature suggests that the 100 μM d_6-ethane plot also exhibits a break, but it is not observed because it is at or slightly below the lowest temperature that can be investigated in aqueous media. The observation of breakpoints for the ethane reaction using DBL2 strongly supports our hypothesis that the Q reaction with substrates occurs in two steps. These experiments show that MMOB mutagenesis can be used to shift the rate-limiting step into the observable temperature range for substrates such as ethane, which give linear Arrhenius plots when using WT-MMOB.

Kinetic Isotope Effect of the Q Decay Reaction and its Temperature Dependence. At any single temperature, the Q

[2] All time courses were better fit with three exponentials than two exponentials especially in the case of ethane or d_6-ethane. Under the conditions used, the k_{QF} is always associated with the positive amplitude and the k_{QD} with the negative amplitude in all fittings for DBL2.

[3] In the sMMO system isolated from *Methylococcus capsulatus* (Bath) the equivalent P intermediate termed H_{peroxo} has been proposed to react with some substrates containing double bonds. However, it is also unreactive with saturated hydrocarbons (*31*).

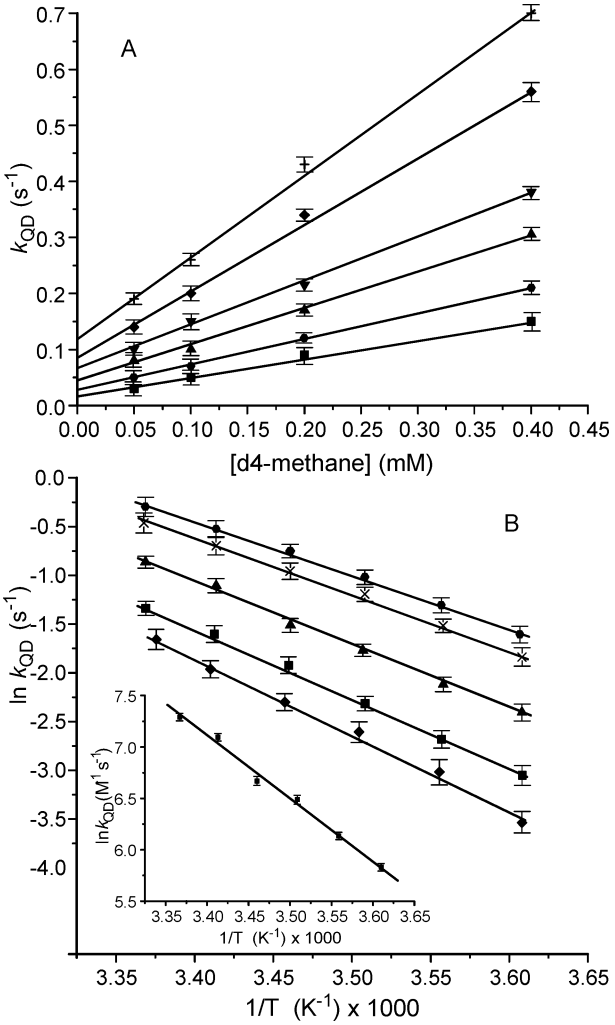

FIGURE 3: Reaction of d_4-methane with Q using DBL2. Panel A: Pseudo first order rate constant for Q decay during a single turnover reaction with d_4-methane. The individual plots from top to bottom represent reactions at 24, 20, 16, 12, 8, and 4 °C. Panel B: Arrhenius plots for the Q decay reaction. From bottom to top, reactions using DBL2 with 50 μM, 100μM, 200 μM, 400 μM, 600 μM d_4-methane. Inset: Arrhenius plots using the second order rate constant for Q decay determined from the slopes of the plots in panel A. Plots of this type were used to determine activation parameters (Table S2) and KIE values (Figure 5).

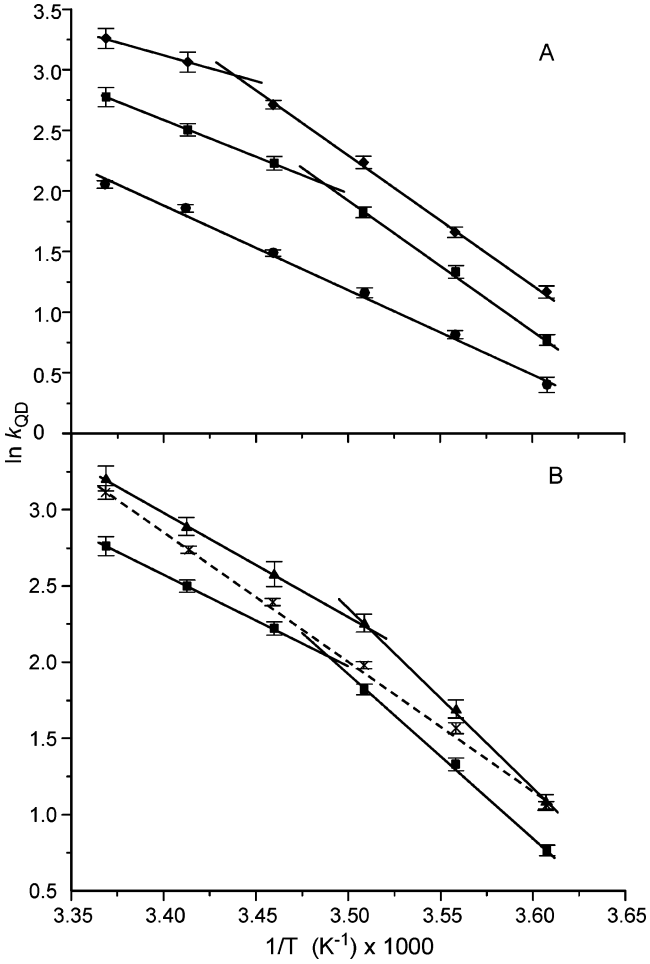

FIGURE 4: Arrhenius plots for the Q decay reaction in the presence of DBL2 and ethane. Panel A: From bottom to top, reactions with d_6-ethane at 100 μM, 200 μM, and 300 μM. Panel B: From bottom to top: Reactions using DBL2 with d_6-ethane, WT-MMOB with ethane (dashed line), and DBL2 with ethane (substrate at 200 μM in each case).

decay reaction appears first order and a plot of the apparent rate constant versus methane concentration is linear (see Figure 3A for example) (*4*). The slope of this plot gives an apparent bimolecular association rate constant. The ratio of these second order Q decay rate constants for the methane and d_4-methane reactions allows a more accurate determination of the deuterium KIE than single concentration measurements. The ln KIEs for the methane reaction using DBL2 or WT-MMOB plotted vs 1/*T* are shown in Figure 5. In both cases, the ln KIEs increase with decreasing temperature part way through the range investigated and then decrease. The magnitude of the KIE at any given temperature is only about half as large for the reactions with DBL2 present. The apparent activation energy for the Q reaction with d_4-methane is about the same as observed when using WT-MMOB (Table S2). Thus, the decreased KIE for the reaction using DBL2 stems primarily from the increased activation energy for the methane reaction. The reactions with ethane as the substrate using DBL2 show a KIE of approximately 1.6 and change little over the temperature range investigated.

DISCUSSION

Our past studies of the temperature dependence of the Q decay rate constant have shown that the reaction with methane consists of at least two steps, nominally assigned as binding and bond cleavage (*24*−*26*). Some past observations suggested that this also applies to other substrates, notably the hyperbolic rather than linear substrate concentration dependence at fixed temperature found for a few relatively poor MMO substrates (*4*, *32*). Nevertheless, for most substrates other than methane one observes (i) a linear rate constant vs substrate concentration plot at any given temperature, (ii) a linear Arrhenius plot, and (iii) no deuterium KIE. These observations are generally indicative of a single step reaction in which a C−H bond is not broken, suggesting that these other substrates react differently than methane with Q. Here we have shown that, through mutagenesis of the regulatory protein MMOB, it is possible to alter the reaction kinetics for ethane oxidation such that both a nonlinear Arrhenius plot and a ^{2}H-KIE are observed. These results suggest that compound Q reacts with alternative substrates using the same general mechanism as is used for

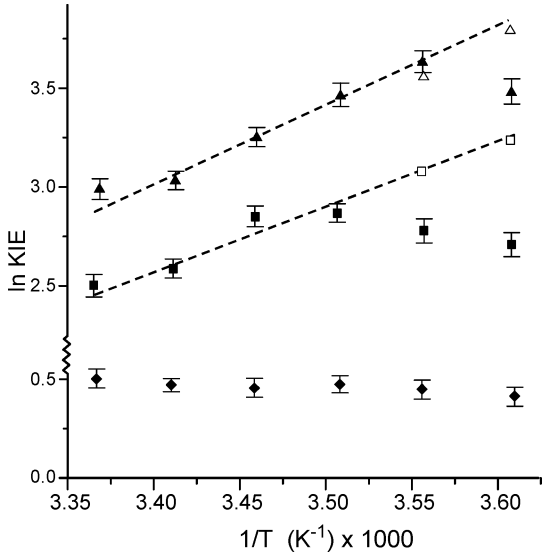

FIGURE 5: Temperature dependence of the KIE. Solid squares represent KIEs of the reaction using DBL2 determined from the ratio of Q decay second order rate constants using normal and deuterated substrates over a range of concentrations (see Figure 3). Open squares represent the predicted KIEs of the reaction using DBL2 and 200 μM substrate concentration based on the first order Q decay rate constant for the normal substrate in the low temperature region extrapolated from the values in the high temperature region where the C−H bond breaking reaction is rate limiting. The triangles represent the corresponding KIEs when using WT-MMOB. Diamonds are the actual KIEs of the reactions using DBL2 and ethane over the temperature range shown. No KIE is observed when using WT-MMOB and ethane.

methane, but the reaction characteristics are normally masked by the nature of the MMOB−MMOH interaction. By unmasking the underlying reaction, its molecular mechanism can potentially be studied. Novel aspects of the reactions with both methane and ethane are revealed by such studies and are discussed here.

Significance of a Break in the Arrhenius Plot for Ethane Oxidation for the Molecular Sieve Hypothesis. The Arrhenius plots for the Q reaction with methane using WT-MMOB (*25*) and those for reactions with methane and ethane using DBL2 are similar in many respects. Plots in each case are nonlinear and show substantial movements in the breakpoint with relatively small changes in substrate concentration. Also, there is a pronounced and linear substrate concentration dependence on the rate constant at any specific temperature in the range of the plots. Together these observations suggest that the individual rate constants of the putative binding and C−H bond breaking reactions are fairly similar such that both contribute substantially to the observed rate constant throughout the observable temperature range.

One implication of the apparently similar binding and C−H bond breaking rates is that even when a break can be observed in the Arrhenius plot, the activation parameters determined from the linear portions will not be purely attributable to just one of the reactions. One indication of this may be in the subtle change in slope seen for the data shown in Figure 3B with increasing substrate concentration. In this experiment, the concentration of d_4-methane causes changes in the relationship of the apparent rate constants for the binding and bond-breaking reactions. If this were purely due to C−H bond breaking, the lines of the Arrhenius plots of d_4-methane at differing concentrations would be all

Scheme 2: Effect of DBL2 on MMOH Active Site Access

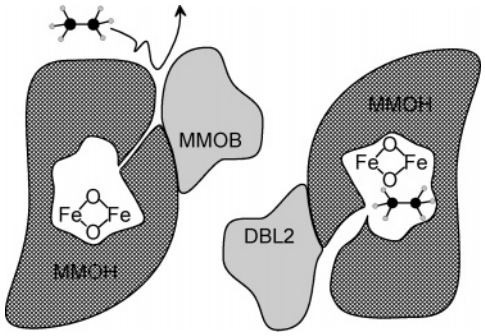

parallel. Nevertheless, the apparent activation parameters can be used to establish trends, and this is used here to reveal the effects of DBL2 on the tunneling component of the reaction coordinate. A second implication is that the binding reactions for methane in the case where WT-MMOB is used, and both methane and ethane reactions where DBL2 is employed, are likely to exhibit high K_d values relative to the concentration of substrate used in the experiments. If this were not the case, then the substrate concentration dependence at specific temperatures in the HTR region would be hyperbolic rather than linear and ultimately disappear at high substrate concentrations.[4] In apparent contradiction to this conclusion, steady state kinetic determinations of the K_m for methane and ethane in the system using WT-MMOB show relatively small values in the low micromolar range (*2*). However, the K_m value also includes rate constants from steps in the hydrocarbon reaction phase. Thus, the rate constants for substrate binding and release are only contributors to the apparent K_m and do not solely determine its value.

For reactions that are rate-limited by C−H bond breaking, one would expect the rate constants for reactions involving methane and ethane to differ by 3 orders of magnitude due to the 4 kcal per mol difference in bond dissociation energy. In previous studies, we have presented evidence that this is indeed the case for the Q reaction with these substrates if the structure of MMOB is altered to allow free access into the active site (*26*). Using WT-MMOB, this large difference in the rate constants is decreased by the combined effects of tunneling in the case of methane and restricted access in the case of ethane. In the study presented here, the breakpoints in the Arrhenius plots for methane and ethane oxidation occur at similar temperatures, suggesting that the relative rates of binding and C−H bond breaking are similar. This implies that DBL2 has a much larger effect on the binding rate of ethane than on that of methane. As illustrated in Scheme 2, one way to rationalize this is to assume that the putative pore into the MMOH active site is sufficiently large in the WT-MMOB−MMOH complex to allow methane to easily enter. Increasing this size will have little effect on the reaction rate. In contrast, ethane is substantially restricted so that the "larger" pore of DBL2 allows ethane to enter the active site much more readily. This brings the binding and C−H bond breaking rate constants closer together and allows the

[4] This conclusion is true so long as the Q reaction with substrates involves only a single substrate molecule. We have argued in the past that another explanation involves two substrate molecules binding at one active site or one molecule binding at each of two active sites in a cooperative manner (*9*). To date, there is no direct evidence for this alternative.

Arrhenius plot break to be observed. Thus, the molecular sieve model accounts well for the experimental observations.

Tunneling. Room temperature quantum tunneling has recently been shown to occur in several biological systems that promote hydrogen transfer either as hydride ions, hydrogen atoms, or protons (see for example refs *33*−*35*). It is not surprising that tunneling can occur in the MMO reaction, but it is remarkable that it is only a large effect in the case of methane oxidation. Thus, more direct evidence for tunneling was sought. Unfortunately, definitive evidence for tunneling in a biological system is difficult to establish because the reaction cannot be followed over a sufficiently large temperature range and comparison of ratios of tritium and deuterium isotope effects in the rate-limiting step often cannot be made. The most easily obtained lines of evidence for the moderate tunneling commonly encountered in a biological system are (*34*) (i) a large ^{2}H-KIE relative to the semiclassical limit of 7−10, (ii) a value for the ratio of the preexponential factors for normal and deuterated substrate less than 0.7, and (iii) a positive slope in the ln ^{2}H-KIE vs 1/*T* plot that is larger that that expected based on the difference in activation energies due solely to the bond dissociation energies for the protium and deuterium forms of the substrate. Some of these criteria can be evaluated in the case of MMO when DBL2 is used.

The ^{2}H-KIE for methane oxidation by Q with DBL2 present is less than that observed when WT-MMOB is used, but it remains significantly larger than the usual limit for a reaction proceeding primarily over the Arrhenius activation barrier. Thus, by this criterion, tunneling still plays a major role in this reaction. The apparent decrease in the tunneling contribution relative to that observed for the reaction using WT-MMOB is unlikely to stem from a difference in the oxygen insertion reaction itself since all substrates give the products normally observed (and the same product distributions for complex substrates). We speculate that the changes in active site structure apparent from spectroscopic studies as MMOB binds to MMOH alter the approach of substrate to the reactive oxygen species in Q, thereby affecting the tunneling contribution. Modifications in MMOB structure seem likely to cause different effects in the MMOH active site structure.

In principle, the preexponential factors for the Q decay reactions using either WT-MMOB or DBL2 could be determined by extrapolation of the Arrhenius plots. However, two factors make this approach unreliable. First, a very limited temperature range is accessible due to the need to work in aqueous media and the presence of a break in the Arrhenius plot. This severely limits the accuracy of the extrapolation to infinite temperature. Second, as noted above, the Arrhenius plots on either side of the break do not reflect pure binding or C−H bond breaking reactions, and this will also be true of the extrapolation.

The plots of the log of the ^{2}H-KIE vs 1/*T* for the methane oxidation reaction using either DBL2 or WT-MMOB shown in Figure 5 are unusual because they exhibit both a positive and a negative slope in the observable temperature range. We believe that this arises because the reaction of methane with Q is rate limited by C−H bond breaking only at high temperatures, whereas C−H bond cleavage is always rate limiting when d_4-methane is the substrate. In order to make a direct comparison of the C−H bond breaking reactions, it is possible to extrapolate the HTR for the methane oxidation Arrhenius plot into the LTR (a specific methane concentration must be assumed). This predicted set of k_{QD} values can then be used to calculate the KIE at temperatures where binding is normally rate limiting. The KIE values using extrapolated rate constants for a reaction with 200 μM methane are plotted in Figure 5 as open symbols. This approach shows that both WT-MMOB and DBL2 reactions exhibit positive slopes with values (3.4−3.6) similar to those found for other systems exhibiting moderate tunneling (2.5−4) (summarized in ref *36*). For comparison, plots for reactions that do not exhibit obvious tunneling effects would be expected to have a slope of about 1.25 if the difference in isotope activation energies is about 2 kcal/mol, as in the case of methane and d_4-methane.

In contrast to methane, the KIE values for ethane reaction with Q using DBL2 show little change with temperature. The small KIE and lack of temperature change do not provide support for a large tunneling contribution in this case.

Conclusion. The efficient and specific oxidation of methane to methanol in a background of potentially more reactive substrates requires the generation of a powerful oxidizing reagent while at the same time controlling which substrates have access to this reagent. The results presented here show for the first time that a nonlinear Arrhenius plot for a reaction occurring at the active site of the hydroxylase component of MMO can be induced by making small changes in the surface residues of the regulatory component. This is strongly supportive of a model in which the powerful reagent of MMO catalysis, compound Q, is protected by a closed protein structure that greatly slows access of substrates. MMOB appears to allow rapid access to methane (and O_2) when it forms a complex with MMOH. We propose that the MMOB surface mutations allow more rapid access to larger substrates, thereby making the access rate constant approach or exceed the C−H bond breaking rate constant as indicated by the nonlinear Arrhenius plot. These results strongly suggest that size selectivity on the order of one methylene group is possible for enzymes. This conclusion is not unlike that reached in the case of systems such as the photoreaction center II, which can differentiate between ammonia and methylamine, apparently due again to restricted access to a buried metal center (*37*, *38*). Similar considerations are also likely to affect numerous biochemical reactions involving small molecules including regulation of intra- and interprotein substrate channeling (*39*−*41*). The precise mechanism of substrate gating in the case of MMOB−MMOH is unknown, but generation of a physical channel sized for methane or induction of an increase in residue mobility at the interface are reasonable possibilities.

SUPPORTING INFORMATION AVAILABLE

Tables of activation parameters for the Q formation and decay reactions in the presence of DBL2 and WT-MMOB. This material is available free of charge via the Internet at http://pubs.acs.org.

REFERENCES

1. Dalton, H. (1980) Oxidation of hydrocarbons by methane monooxygenase from a variety of microbes, *Adv. Appl. Microbiol. 26*, 71−87.

2. Fox, B. G., Froland, W. A., Dege, J. E., and Lipscomb, J. D. (1989) Methane monooxygenase from *Methylosinus trichosporium* OB3b. Purification and properties of a three-component system with high specific activity from a type II methanotroph, *J. Biol. Chem. 264*, 10023−10033.
3. Fox, B. G., Surerus, K. K., Münck, E., and Lipscomb, J. D. (1988) Evidence for a μ-oxo-bridged binuclear iron cluster in the hydroxylase component of methane monooxygenase. Mössbauer and EPR studies, *J. Biol. Chem. 263*, 10553−10556.
4. Lee, S.-K., Nesheim, J. C., and Lipscomb, J. D. (1993) Transient intermediates of the methane monooxygenase catalytic cycle, *J. Biol. Chem. 268*, 21569−21577.
5. Elango, N., Radhakrishnan, R., Froland, W. A., Wallar, B. J., Earhart, C. A., Lipscomb, J. D., and Ohlendorf, D. H. (1997) Crystal structure of the hydroxylase component of methane monooxygenase from *Methylosinus trichosporium* OB3b, *Protein Sci. 6*, 556−568.
6. Fox, B. G., Liu, Y., Dege, J. E., and Lipscomb, J. D. (1991) Complex formation between the protein components of methane monooxygenase from *Methylosinus trichosporium* OB3b. Identification of sites of component interaction, *J. Biol. Chem. 266*, 540−550.
7. Liu, K. E., Wang, D., Huynh, B. H., Edmondson, D. E., Salifoglou, A., and Lippard, S. J. (1994) Spectroscopic detection of intermediates in the reaction of dioxygen with the reduced methane monooxygenase hydroxylase from *Methylococcus capsulatus* (Bath), *J. Am. Chem. Soc. 116*, 7465−7466.
8. Liu, Y., Nesheim, J. C., Lee, S.-K., and Lipscomb, J. D. (1995) Gating effects of component B on oxygen activation by the methane monooxygenase hydroxylase component, *J. Biol. Chem. 270*, 24662−24665.
9. Brazeau, B. J., and Lipscomb, J. D. (2000) Kinetics and activation thermodynamics of methane monooxygenase compound Q formation and reaction with substrates, *Biochemistry 39*, 13503−13515.
10. Fox, B. G., Borneman, J. G., Wackett, L. P., and Lipscomb, J. D. (1990) Haloalkene oxidation by the soluble methane monooxygenase from *Methylosinus trichosporium* OB3b: mechanistic and environmental implications, *Biochemistry 29*, 6419−6427.
11. Wallar, B. J., and Lipscomb, J. D. (1996) Dioxygen activation by enzymes containing binuclear non-heme iron clusters, *Chem. Rev. 96*, 2625−2657.
12. Feig, A. L., and Lippard, S. J. (1994) Reactions of non-heme iron(II) centers with dioxygen in biology and chemistry, *Chem. Rev. 94*, 759−805.
13. Paulsen, K. E., Liu, Y., Fox, B. G., Lipscomb, J. D., Münck, E., and Stankovich, M. T. (1994) Oxidation-reduction potentials of the methane monooxygenase hydroxylase component from *Methylosinus trichosporium* OB3b, *Biochemistry 33*, 713−722.
14. Liu, K. E., and Lippard, S. J. (1991) Redox properties of the hydroxylase component of methane monooxygenase from *Methylococcus capsulatus* (Bath). Effects of protein B, reductase, and substrate, *J. Biol. Chem. 266*, 12836−12839.
15. Froland, W. A., Andersson, K. K., Lee, S.-K., Liu, Y., and Lipscomb, J. D. (1992) Methane monooxygenase component B and reductase alter the regioselectivity of the hydroxylase component-catalyzed reactions. A novel role for protein-protein interactions in an oxygenase mechanism, *J. Biol. Chem. 267*, 17588−17597.
16. Rosenzweig, A. C., Frederick, C. A., Lippard, S. J., and Nordlund, P. (1993) Crystal structure of a bacterial non-haem iron hydroxylase that catalyses the biological oxidation of methane, *Nature 366*, 537−543.
17. Rosenzweig, A. C., Nordlund, P., Takahara, P. M., Frederick, C. A., and Lippard, S. J. (1995) Geometry of the soluble methane monooxygenase catalytic diiron center in two oxidation states, *Chem. Biol. 2*, 409−418.
18. Whittington, D. A., Rosenzweig, A. C., Frederick, C. A., and Lippard, S. J. (2001) Xenon and halogenated alkanes track putative substrate binding cavities in the soluble methane monooxygenase hydroxylase, *Biochemistry 40*, 3476−3482.
19. Hendrich, M. P., Münck, E., Fox, B. G., and Lipscomb, J. D. (1990) Integer-spin EPR studies of the fully reduced methane monooxygenase hydroxylase component, *J. Am. Chem. Soc. 112*, 5861−5865.
20. Pulver, S. C., Froland, W. A., Lipscomb, J. D., and Solomon, E. I. (1997) Ligand field circular dichroism and magnetic circular dichroism studies of component B and substrate binding to the hydroxylase component of methane monooxygenase, *J. Am. Chem. Soc. 119*, 387−395.
21. Chang, S. L., Wallar, B. J., Lipscomb, J. D., and Mayo, K. H. (1999) Solution structure of component B from methane monooxygenase derived through heteronuclear NMR and molecular modeling, *Biochemistry 38*, 5799−5812.
22. Chang, S. L., Wallar, B. J., Lipscomb, J. D., and Mayo, K. H. (2001) Residues in *Methylosinus trichosporium* OB3b methane monooxygenase component B involved in molecular interactions with reduced- and oxidized-hydroxylase component: a role for the N-terminus, *Biochemistry 40*, 9539−9551.
23. Walters, K. J., Gassner, G. T., Lippard, S. J., and Wagner, G. (1999) Structure of the soluble methane monooxygenase regulatory protein B, *Proc. Natl. Acad. Sci. U.S.A. 96*, 7877−7882.
24. Wallar, B. J., and Lipscomb, J. D. (2001) Methane monooxygenase component B mutants alter the kinetics of steps throughout the catalytic cycle, *Biochemistry 40*, 2220−2233.
25. Brazeau, B. J., Wallar, B. J., and Lipscomb, J. D. (2001) Unmasking of deuterium kinetic isotope effects on the methane monooxygenase compound Q reaction by site-directed mutagenesis of component B, *J. Am. Chem. Soc. 123*, 10421−10422.
26. Brazeau, B. J., and Lipscomb, J. D. (2003) Key amino acid residues in the regulation of soluble methane monooxygenase catalysis by component B, *Biochemistry 42*, 5618−5631.
27. Nesheim, J. C., and Lipscomb, J. D. (1996) Large isotope effects in methane oxidation catalyzed by methane monooxygenase: evidence for C−H bond cleavage in a reaction cycle intermediate, *Biochemistry 35*, 10240−10247.
28. Fox, B. G., Froland, W. A., Jollie, D. R., and Lipscomb, J. D. (1990) Methane monooxygenase from *Methylosinus trichosporium* OB3b, *Methods Enzymol. 188*, 191−202.
29. Shu, L., Nesheim, J. C., Kauffmann, K., Münck, E., Lipscomb, J. D., and Que, L., Jr. (1997) An $Fe(IV)_2O_2$ diamond core structure for the key intermediate Q of methane monooxygenase, *Science 275*, 515−518.
30. Lee, S.-K., Fox, B. G., Froland, W. A., Lipscomb, J. D., and Münck, E. (1993) A transient intermediate of the methane monooxygenase catalytic cycle containing a $Fe^{IV}Fe^{IV}$ cluster, *J. Am. Chem. Soc. 115*, 6450−6451.
31. Beauvais, L. G., and Lippard, S. J. (2005) Reactions of the peroxo intermediate of soluble methane monooxygenase hydroxylase with ethers, *J. Am. Chem. Soc. 127*, 7370−7378.
32. Ambundo, E. A., Friesner, R. A., and Lippard, S. J. (2002) Reactions of methane monooxygenase intermediate Q with derivatized methanes, *J. Am. Chem. Soc. 124*, 8770−8771.
33. Kohen, A., Cannio, R., Bartolucci, S., and Klinman, J. P. (1999) Enzyme dynamics and hydrogen tunnelling in a thermophilic alcohol dehydrogenase, *Nature 399*, 496−499.
34. Kohen, A., and Klinman, J. P. (1999) Hydrogen tunneling in biology, *Chem. Biol. 6*, 191−197.
35. Liang, Z.-X., and Klinman, J. P. (2004) Structural bases of hydrogen tunneling in enzymes: progress and puzzles, *Curr. Opin. Struct. Biol. 14*, 648−655.
36. Siebrand, W., and Smedarchina, Z. (2006) Mechanism of CH-bond cleavage catalyzed by enzymes, in *Isotope effects in chemistry and biology* (Kohen, A., and Limbach, H.-H., Eds.) pp 725−741, Taylor & Francis, Boca Raton, FL.
37. Ouellette, A. J. A., Anderson, L. B., and Barry, B. A. (1998) Amine binding and oxidation at the catalytic site for photosynthetic water oxidation, *Proc. Natl. Acad. Sci. U.S.A. 95*, 2204−2209.
38. Beck, W. F., and Brudvig, G. W. (1988) Resolution of the paradox of ammonia and hydroxylamine as substrate analogs for the water-oxidation reaction catalyzed by photosystem II, *J. Am. Chem. Soc. 110*, 1517−1523.
39. Raushel, F. M., Thoden, J. B., and Holden, H. M. (2003) Enzymes with molecular tunnels, *Acc. Chem. Res. 36*, 539−548.
40. Seravalli, J., and Ragsdale, S. W. (2000) Channeling of carbon monoxide during anaerobic carbon dioxide fixation, *Biochemistry 39*, 1274−1277.
41. Lindahl, P. A. (2002) The Ni-containing carbon monoxide dehydrogenase family: light at the end of the tunnel?, *Biochemistry 41*, 2097−2105.

BI051605G